JOURNAL OF SOLID STATE CHEMISTRY **122,** 151–159 (1996)
ARTICLE NO. 0096

Characterization of the Structure of $LaD_{2.50}$ by Neutron Powder Diffraction

T. J. Udovic,* Q. Huang,*,† and J. J. Rush*

*Materials Science and Engineering Laboratory, National Institute of Standards and Technology, Gaithersburg, Maryland 20899; and †Department of Materials and Nuclear Engineering, University of Maryland, College Park, Maryland 20742

Received July 12, 1995; in revised form November 7, 1995; accepted November 15, 1995

Neutron powder diffraction (NPD) measurements of the rare-earth deuteride $LaD_{2.50}$ were undertaken between 10 and 430 K. Rietveld refinements indicated that, above ~385 K, the $LaD_{2.50}$ structure is cubic (*Fm*3*m*) with deuterium fully occupying the tetrahedral (t) interstices of the fcc La lattice and the excess deuterium occupying a portion of the octahedral (o) interstices with full statistical disorder. As the temperature is decreased below ~385 K, the $LaD_{2.50}$ structure undergoes a tetragonal distortion concomitant with the onset of deuterium long-range order (*I*4$_1$/*amd*) in the o sublattice, similar to previous structural results for the light-rare-earth deuterides RD_{2+x} for $0.3 < x < 0.5$. Fully developed long-range order is established in the vicinity of 200 to 230 K. Considering the o sublattice as residing in a family of $(042)_{Cubic}$ planes, perfect long-range order can be described as a repeating four-plane sequence comprised of two consecutive planes possessing fully occupied o sites followed by two consecutive planes possessing fully vacant o sites. This ordering is accompanied by correlated basal-plane displacements of the t-site deuterium atoms along either the *a* or *b* axes in response to repulsive interactions with the nearest-neighbor D_o atoms. Moreover, the *c*-directed La–D_o bond distances are decreased by a displacement of the La atoms toward the D_o atoms.

INTRODUCTION

The light-rare-earth metal hydrides RH_{2+x} (where *R* represents La, Ce, Pr, and Nd) possess a nominally fcc metal lattice over a wide concentration region of $0 \le x \le x_{max}$. For LaH_{2+x} and CeH_{2+x}, $x_{max} \approx 1$ (1), whereas for NdH_{2+x}, $x_{max} \approx 0.65$–0.7 (2, 3). Although it has been generally assumed that $x_{max} \approx 1$ also for PrH_{2+x} (4), a comparison of pressure-concentration isotherms (3) for PrH_{2+x} and NdH_{2+x} has suggested that the precipitation of a NdH_3-like metal-trihydride phase may occur above $x \approx 0.7$ for PrH_{2+x}. Within the RH_{2+x} fcc structure, two H atoms per *R* atom fully occupy the tetrahedral (t) interstices. The *x* additional H atoms per *R* atom reside in the octahedral (o) interstices. Tentative phase diagrams (1) constructed for LaH_{2+x} and CeH_{2+x} illustrate an array of concentration- and temperature-dependent phase transitions known to involve tetragonal lattice distortion and o-site hydrogen (H_o) ordering. For example, we recently performed a neutron powder diffraction (NPD) study (5) of $LaD_{2.25}$ confirming the presence of a high-temperature cubic *Fm*3*m* structure (with full D_o disorder) which undergoes tetragonal distortion below ~345 K to form a low-temperature *I*4/*mmm* structure (with long-range D_o ordering). Similar structural behavior was also observed for $CeD_{2.26}$ (6) and the heavy-rare-earth deuterides TbD_{2+x} for $0.1 \le x \le 0.25$ (7, 8). Considering all o sites in the fcc metal lattice as residing in a family of $(042)_C$ planes, perfect *I*4/*mmm* order corresponded to full o-site occupation for every fourth (042) plane with all other (042) planes empty. (In this paper, cubic indices are designated by either the subscript C or no subscript; tetragonal indices are designated by the subscript T).

Various NPD studies have indicated that a different RD_{2+x} ordered structure exists for $\sim 0.3 < x \le 0.5$. Room-temperature NPD measurements (9) of $LaD_{2.30}$, $PrD_{2.37}$, $CeD_{2.29}$, and $CeD_{2.51}$ pointed to the presence of D_o long-range order with tetragonal *I*4$_1$*md* symmetry for the former three compounds and the absence of D_o long-range order with cubic *Fm*3*m* symmetry for the latter compound, although sample homogeneity and stoichiometric accuracy in this early study may have been compromised by metal impurities and synthesis methods used. Later room-temperature NPD measurements of $CeD_{2.43}$ (1, 6) and $NdD_{2.36}$ (10) also inferred *I*4$_1$*md*-ordered structures. Temperature-dependent NPD data (11) reported for $CeD_{2.45}$ corroborated a slightly higher *I*4$_1$/*amd* symmetry for the ordered structure. In all these studies, perfect *I*4$_1$*md* (or *I*4$_1$/*amd*) order corresponded to a repeating sequence of four (042) planes comprised of two consecutive planes possessing fully occupied o sites followed by two consecutive planes possessing fully vacant o sites.

It is of interest to extend these RD_{2+x} structural studies to include the ordering behavior in the LaD_{2+x} system near $x = 0.5$, which is the D concentration corresponding to perfect *I*4$_1$*md* (or *I*4$_1$/*amd*) order. In the present paper,

0022-4596/96 $18.00

we report the results of a detailed NPD study concerning the temperature-dependent structure of $LaD_{2.50}$. This study is part of our general efforts to elucidate the true structural details of the different phases typically present in the light-rare-earth phase diagrams.

EXPERIMENTAL PROCEDURE

Synthesis of the $LaD_{2.50}$ sample followed a two-step procedure similar to that used for preparing $LaD_{2.25}$ (5). In the first step at 773 K, ~27 g of high-purity La (99.99 at.% metal purity, Johnson Matthey[1]) were loaded with D_2 (Spectra Gases Research Grade) by gas-phase absorption in a quartz tube to a nominal D/La stoichiometry of 2.00, allowed to equilibrate for 19 h, and finally evacuated for 9 h to remove any existing D_o atoms, which are known to be unstable at this temperature (12), thus forming the "ideal" $RD_{2.00}$ baseline stoichiometry (i.e., the fluorite structure) with only t-site deuterium (D_t) atoms present (13). In the second step, the pure dideuteride sample was loaded with additional D_2 at 773 K to form the superstoichiometric $LaD_{2.50}$ compound, was allowed to cool slowly over a 5-h period to 453 K followed by a 12-h equilibration, and was further cooled over a 3-h period to 377 K followed by an additional 3-h equilibration. Finally, the insignificant D_2 vapor pressure above the sample was evacuated, while the sample was rapidly cooled to room temperature. With this procedure, the uncertainty in the targeted x value was estimated to be ± 0.01–0.02. The sample was then transferred to a He-filled glove box, pulverized, and sealed in a cylindrical V tube (12 mm inner dia. × 50 mm ht.) for NPD measurements up to 375 K. An additional 430-K powder pattern was measured after transferring and sealing the sample in a cylindrical Al tube (15 mm inner dia. × 40 mm ht.). During experiments, the sample was mounted in a temperature-controlled, closed-cycle He refrigerator.

All NPD measurements were performed at the Neutron Beam Split-Core Reactor (NBSR) at the National Institute of Standards and Technology (NIST) using the high-resolution, 32-counter BT-1 diffractometer (14). The Cu(311) monochromator was used at a wavelength of 1.5391(1) Å. The wavelength was calibrated using an Al_2O_3 standard. The horizontal divergences were 15′, 20′, and 7′ of arc for the in-pile, monochromatic-beam, and diffracted-beam collimators, respectively. Data were collected every 0.05° over a 2θ angular range of 4.5° to 165°, although no Bragg features were evident below 17°. All refinements were carried out with the Rietveld method (15) using the program GSAS (16). Neutron-scattering amplitudes used in the refinements were 8.27 fm for La and 6.67 fm for D (16). The standard uncertainty (i.e., the estimated standard deviation) for the wavelength calibration was not propagated to the estimates for the cell parameters and other reported Rietveld results.

[1] Manufacturers are identified in order to provide complete identification of experimental conditions, and such identification is not intended as a recommendation or endorsement by the NIST.

DISCUSSION OF THE STRUCTURAL RESULTS

Neutron diffraction measurements were performed between 10 and 430 K. Figure 1 illustrates characteristic high- and low-temperature powder patterns. The powder patterns for the V-contained sample indicated four small temperature-independent peaks unable to be indexed using the calculated lattice parameters. These peaks were less than 2% as intense as the strongest lattice reflection. Two of the peaks were most likely due to $\lambda/2$ wavelength contamination; the other two were attributed to some unknown impurity unrelated to the sample. All four peaks were excluded from the refinements. In addition, the small Bragg peaks due to the Al sample container at 430 K were also excluded from the refinements.

Tables 1–3 summarize the refinement results. In particular, the high-temperature pattern at 430 K was successfully refined using the cubic symmetry of the *Fm*3*m* (No. 225) space group, in accordance with previous RH_{2+x} structural studies (5, 11, 17). The La atoms were located at 4*a* (0, 0, 0), D_t atoms at 8*c* ($\frac{1}{4}$, $\frac{1}{4}$, $\frac{1}{4}$), and D_o atoms disordered over the sites 4*b* ($\frac{1}{2}$, $\frac{1}{2}$, $\frac{1}{2}$). The refinement with this model gave good agreement parameters R_p = 5.90%, R_{wp} = 7.52%, and χ = 1.30, a lattice constant a_C = 5.63639(7) Å, and isotropic temperature factors (B) of 0.81(4), 1.93(7), and 3.9(3) Å^2 for the La, D_t, and D_o atoms, respectively. At 375 K and below, some peaks showed splitting and additional weak superlattice peaks appeared. All lines readily indexed using an enlarged tetragonal unit cell with $a_T = a_C$ and $c_T \approx 2a_C$. This low-temperature tetragonal $LaD_{2.50}$ phase was successfully refined using the symmetry of the $I4_1/amd$ (No. 141) space group, in line with the more-recent $CeD_{2.45}$ structural study (11). In this structure, the La atoms were located at 8*e* (0, 0, z); the D_t atoms were located at the D(t) position 16*f* (x, $\frac{1}{4}$, $\frac{1}{8}$), and the D_o atoms were split into D(o1) at 4*a* (0, 0, 0) and D(o2) at 4*b* (0, 0, $\frac{1}{2}$). Using the 10-K data to exemplify the low-temperature structure, the refinement results yielded the agreement parameters R_p = 6.15%, R_{wp} = 7.93%, and χ = 1.81, the lattice constants a_T = 5.59234(9)) Å and c_T = 11.2907(2) Å, the atomic coordinates z = 0.7540(1) for La and x = 0.2682(3) for D(t), the occupancy parameters $n_{D(t)}$ = 1.00(1), $n_{D(o1)}$ = 0.91(1), and $n_{D(o2)}$ = 0.03(1), and the temperature factors B_{La} = 0.05(3) Å^2, $B_{D(t)}$ = 0.96(5) Å^2, and $B_{D(o1)} = B_{D(o2)}$ = 2.0(1) Å^2. The relatively large temperature factor for the D_o atoms compared with that for the D_t atoms is reminiscent of that observed for $LaD_{2.25}$ (5) and most likely reflects the larger size of the

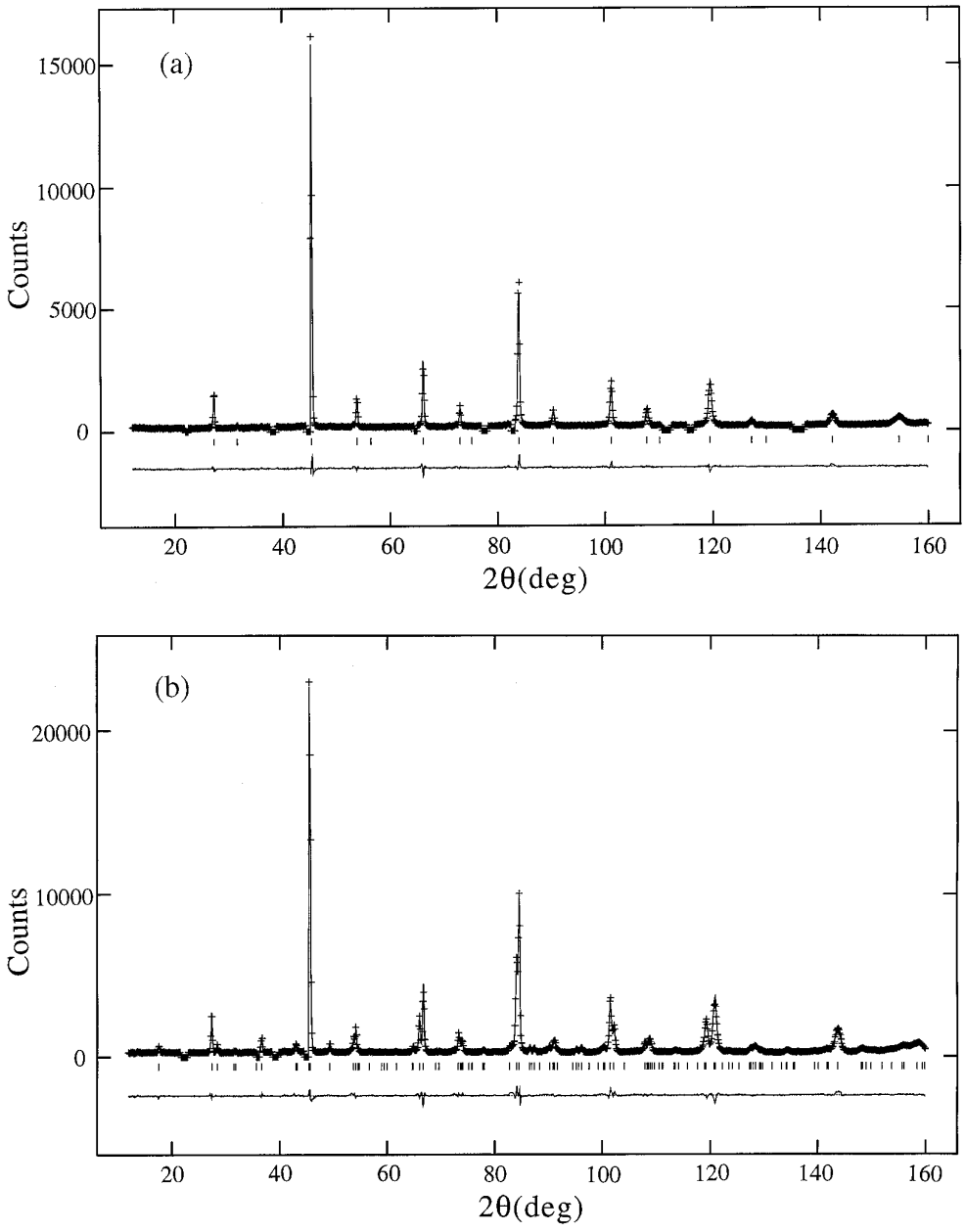

FIG. 1. (a) Cubic high-temperature (430 K, *Fm*3*m*) and (b) tetragonal low-temperature (10 K, $I4_1/amd$) neutron powder diffraction patterns and corresponding fits (solid lines) for $LaD_{2.50}$. Below each data set is the difference pattern between calculated and observed intensities as well as a series of vertical lines to mark the calculated positions of Bragg reflections. The fits indicate excluded regions, which are described in the text.

o sites compared to the t sites. For comparison with the isotropic temperature factors, a modified refinement model that used an anisotropic D_o temperature factor yielded B_{11}, B_{22}, and B_{33} values of 2.0(1), 2.0(1), and 1.9(1) Å^2, respectively. The moderate temperature dependence of the D_o temperature factor (which varies from 2.0(1) Å^2 at 10 K to 4.2(3) Å^2 at 375 K, and 3.9(3) Å^2 for the cubic structure at 430 K) suggests that the large factors reflect a large thermal motion of centered o-site atoms rather than positional disorder due to distinct off-center D_o displacements. Such positional disorder would more likely be reflected by a weaker temperature dependence of the temperature factor. This conclusion is somewhat contrary to the earlier NPD studies of RD_{2+x} (9, 18–20) where it was suggested that the D_o atoms were displaced along the [111] directions. One might argue that such displacements may very well be energetically favorable (21), since they bring the D_o atoms into closer bonding proximity with

TABLE 1
Lattice Parameters for $LaD_{2.50}$, Space Group: $I4_1/amd$ (No. 141)

T(K)	a_T(Å)	c_T(Å)	V(Å^3)	$c_T/(2a_T)$	R_p(%)	R_{wp}(%)	χ
10	5.59234(9)	11.2907(2)	353.11(1)	1.00948(3)	6.15	7.93	1.81
100	5.59282(9)	11.2914(2)	353.19(2)	1.00945(4)	6.64	8.57	1.36
150	5.59468(9)	11.2938(2)	353.50(2)	1.00933(4)	6.50	8.21	1.30
200	5.5990(1)	11.2951(2)	354.09(2)	1.00867(4)	6.46	8.21	1.28
250	5.60388(9)	11.2923(2)	354.62(2)	1.00754(4)	6.14	7.92	1.23
258	5.6051(1)	11.2912(3)	354.73(2)	1.00723(4)	7.50	9.64	1.06
260	5.6053(1)	11.2913(3)	354.76(2)	1.00720(4)	7.42	9.66	1.06
262	5.6055(1)	11.2906(3)	354.77(2)	1.00710(4)	7.43	9.49	1.05
264	5.6057(1)	11.2904(3)	354.79(2)	1.00705(4)	7.39	9.48	1.04
266	5.6060(1)	11.2902(3)	354.82(2)	1.00697(4)	7.56	9.46	1.06
268	5.6064(1)	11.2899(3)	354.86(2)	1.00688(4)	7.40	9.53	1.05
270	5.6069(1)	11.2897(2)	354.92(2)	1.00677(4)	6.27	8.10	1.26
300	5.61101(8)	11.2853(2)	355.30(2)	1.00564(3)	5.27	6.78	1.40
320	5.6139(1)	11.2827(3)	355.58(2)	1.00489(4)	6.26	7.93	1.24
340	5.61833(9)	11.2782(3)	356.00(2)	1.00370(5)	5.56	7.10	1.58
350	5.6194(1)	11.2732(3)	355.97(2)	1.00306(5)	6.45	8.05	1.25
360	5.6217(1)	11.2703(4)	356.18(2)	1.00239(6)	6.34	8.02	1.22
375	5.6243(1)	11.2704(4)	356.18(2)	1.00194(6)	6.01	7.68	1.19
430[a]	5.63639(7) = a_C = c_C		178.872(7)		5.90	7.52	1.30

[a] Space group: $Fm3m$ (No. 225).

TABLE 2
Atomic Parameters for $LaD_{2.50}$, Space Group: $I4_1/amd$ (No. 141) with Atomic Positions La at 8*e* (0, 0, *z*), D(t) at 16*f* (*x*, ¼, ⅛), D(o1) at 4*a* (0, 0, 0), and D(o2) at 4*b* (0, 0, ½)[a]

	La		D(t)			D(o1)		D(o2)	
T(K)	z	B(Å^2)	x	B(Å^2)	n	B(Å^2)	n	n	D/La
10	0.7540(1)	0.05(3)	0.2682(3)	0.96(5)	1.00(1)	2.0(1)	0.91(1)	0.03(1)	2.47(3)
100	0.7541(2)	0.12(3)	0.2683(3)	1.01(6)	1.00(1)	1.9(1)	0.90(1)	0.03(1)	2.47(3)
150	0.7538(2)	0.17(4)	0.2685(3)	1.04(6)	1.00(1)	2.1(1)	0.92(1)	0.03(1)	2.48(3)
200	0.7538(2)	0.26(4)	0.2680(3)	1.10(6)	1.01(1)	2.3(2)	0.90(1)	0.04(1)	2.49(3)
250	0.7535(2)	0.38(4)	0.2676(3)	1.24(6)	1.00(1)	2.5(2)	0.90(1)	0.06(1)	2.48(3)
258	0.7538(2)	0.37(4)	0.2675(3)	1.32(7)	1.01(1)	2.4(2)	0.88(1)	0.07(1)	2.50(3)
260	0.7537(2)	0.34(5)	0.2676(3)	1.34(7)	1.01(1)	2.4(2)	0.86(1)	0.08(1)	2.49(3)
262	0.7538(2)	0.32(4)	0.2673(4)	1.36(8)	1.01(1)	2.3(2)	0.88(1)	0.06(1)	2.49(3)
264	0.7535(2)	0.37(4)	0.2679(3)	1.25(7)	1.01(1)	2.6(2)	0.87(1)	0.07(1)	2.49(3)
266	0.7538(2)	0.41(5)	0.2676(4)	1.28(7)	0.99(2)	2.6(2)	0.88(1)	0.09(1)	2.47(3)
268	0.7535(2)	0.36(5)	0.2673(3)	1.36(8)	1.01(1)	2.3(2)	0.85(1)	0.08(1)	2.48(3)
270	0.7537(2)	0.41(4)	0.2679(3)	1.30(6)	1.00(1)	2.8(2)	0.88(1)	0.09(1)	2.49(3)
300	0.7536(2)	0.45(3)	0.2660(3)	1.40(6)	1.01(1)	2.8(2)	0.86(1)	0.10(1)	2.50(3)
320	0.7534(2)	0.56(4)	0.2657(3)	1.42(7)	0.99(1)	3.2(2)	0.83(1)	0.15(1)	2.48(3)
340	0.7529(2)	0.66(4)	0.2632(4)	1.45(5)	1.01(1)	3.6(2)	0.78(1)	0.20(1)	2.51(3)
350	0.7528(3)	0.61(4)	0.2616(4)	1.57(6)	0.97(1)	3.1(2)	0.72(2)	0.25(1)	2.43(4)
360	0.7518(4)	0.79(5)	0.2581(6)	1.53(7)	0.98(1)	3.9(3)	0.67(2)	0.33(2)	2.46(4)
375	0.7505(8)	0.81(5)	0.2538(12)	1.58(8)	0.99(1)	4.2(3)	0.59(3)	0.41(3)	2.48(5)
430[b]		0.81(4)		1.93(7)	0.98(1)	3.9(3)	0.48(1)		2.46(3)

[a] Constraints: $n_{La} = 1$, $B_{D(o1)} = B_{D(o2)}$.
[b] Space group: $Fm3m$ (No. 225); atomic positions: La at 4*a* (0, 0, 0), D(t) at 8*c* (¼, ¼, ¼), and D(o) at 4*b* (½, ½, ½).

TABLE 3
Selected Interatomic Distances for $LaD_{2.50}$ Determined from the Refinement Models Described in the Text

T(K)	D(o1)–La ×2	D(o1)–La ×4	D(o2)–La ×2	D(o2)–La ×4	D(t)–La ×2	D(t)–La ×2
10	2.777(2)	2.79654(5)	2.868(2)	2.79654(5)	2.400(1)	2.464(1)
100	2.777(2)	2.79679(5)	2.869(2)	2.79679(5)	2.400(1)	2.464(1)
150	2.780(2)	2.79767(5)	2.867(2)	2.79767(5)	2.398(1)	2.467(1)
200	2.781(2)	2.79984(6)	2.867(2)	2.79984(6)	2.401(1)	2.467(1)
250	2.784(2)	2.80221(5)	2.862(2)	2.80221(5)	2.401(1)	2.469(2)
258	2.780(2)	2.80285(7)	2.865(2)	2.80285(7)	2.403(2)	2.467(2)
260	2.782(2)	2.80294(7)	2.864(2)	2.80294(7)	2.402(2)	2.468(2)
262	2.780(2)	2.80306(7)	2.865(2)	2.80306(7)	2.404(2)	2.466(2)
264	2.783(2)	2.80315(6)	2.863(2)	2.80315(6)	2.406(2)	2.470(2)
266	2.780(2)	2.80331(7)	2.865(2)	2.80331(7)	2.403(2)	2.467(2)
268	2.784(2)	2.80348(6)	2.862(2)	2.80348(6)	2.402(2)	2.469(2)
270	2.781(2)	2.80377(6)	2.864(2)	2.80377(6)	2.402(2)	2.469(2)
300	2.781(2)	2.80580(5)	2.862(2)	2.80580(5)	2.408(2)	2.464(2)
320	2.782(2)	2.80722(6)	2.860(2)	2.80722(6)	2.409(2)	2.465(2)
340	2.787(2)	2.80935(5)	2.852(2)	2.80935(5)	2.413(2)	2.461(2)
350	2.786(3)	2.80986(6)	2.850(3)	2.80986(6)	2.418(3)	2.456(3)
360	2.798(4)	2.81091(6)	2.837(4)	2.81091(6)	2.422(4)	2.452(4)
375	2.812(9)	2.81214(6)	2.823(9)	2.81214(6)	2.428(7)	2.446(7)

T(K)	D(o)–La ×6	D(t)–La ×4
430	2.81720(4)	2.43976(2)

three of the nearest-neighbor La atoms. Yet, neutron spectroscopic measurements (22–24) of the optic-vibrational density of states of H_o and D_o atoms in $R(H/D)_{2+x}$ are more in line with the presence of centered o-site atoms. The apparent large thermal motion of the D_o atoms may very well reflect some o-site disorder where the distribution of D nuclear density is maximized at the o-site center.

Attempts to refine the data using the $I4_1md$ (No. 109) space group (i.e., removing the glide plane symmetry operation) as in the early NPD results (6, 9) meant splitting the $I4_1/amd$ positions for La, D(t), D(o1), and D(o2). This resulted in very high correlations between the split positions of the different atoms, which strongly suggested that the higher symmetry $I4_1/amd$ space group better described the actual structure of the low-temperature ordered phase.

Schematics of the $LaD_{2.50}$ structure at high and low temperature are illustrated in Fig. 2. Figure 2a shows the unit cell representing the high-temperature fluorite structure with full cubic symmetry and randomly occupied o sites. Figure 2b shows the doubled unit cell of the low-temperature perfectly ordered structure. In the D_o sublattice, all D(o1) sites are occupied, while all D(o2) sites are vacant. Arrows indicate that the La atoms are shifted in the c direction toward the occupied D(o1) sites. Since all La atoms have only one nearest-neighbor D_o atom, they are expected to relax toward the D_o atom to lower the system energy (25), as was observed for $LaD_{2.25}$ (5). Moreover, arrows also indicate that the D_t atoms are shifted away from the t-site center in a correlated fashion along either the a or b directions. The D_t-displacement vectors appear to be determined by repulsive D_o–D_t interactions involving the two nearest-neighbor D_o atoms associated with each D_t atom. Such interactions were also observed for $LaD_{2.25}$ (5). These La and D(t) site displacements are similar to those reported (6, 9, 11) for the related light-rare-earth deuterides.

Figure 2c illustrates the (042) [or equivalent $(044)_T$] planes that define the o sublattice, each plane labelled by the type of o site that it contains. In this way, the o sublattice can be described as a repeating series of four (042) planes in the order –D(o1)–D(o1)–D(o2)–D(o2)–. In the perfectly ordered state, only the D(o1) planes are occupied. Of the twelve nearest-neighbor o sites surrounding each D_o atom, there are four occupied D(o1) and eight unoccupied D(o2) sites; hence, two-thirds of the nearest-neighbor o sites are vacant. This should be compared to the $I4/mmm$ ordering in $LaD_{2.25}$ (5), where only every fourth (042) plane is occupied. In this latter case, all nearest-neighbor o sites are vacant, an observation which has prompted others (7, 26) to suggest that a repulsive interaction between D_o atoms drives the D_o ordering in these systems.

A comparison of the D_o ordering in the o sublattices of $LaD_{2.25}$ and $LaD_{2.50}$ is shown in Fig. 3 alongside the vacant and fully occupied o sublattices of LaD_2 and LaD_3. The

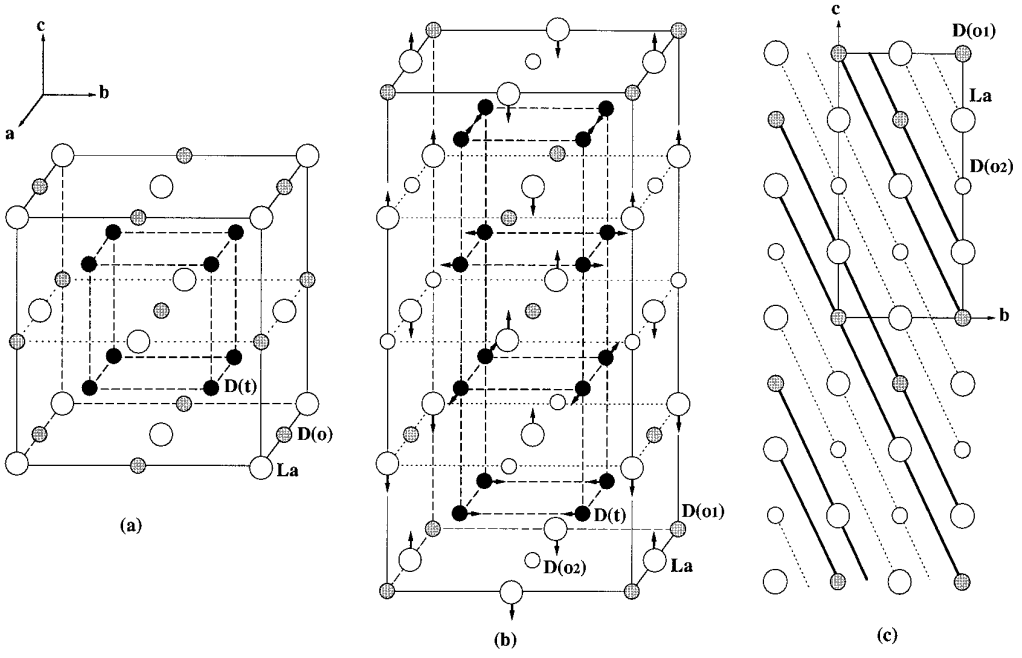

FIG. 2. Schematic of the $LaD_{2.50}$ structure at (a) high temperature ($Fm3m$) and (b) low temperature ($I4_1/amd$); arrows indicate the displacement directions of the D_t and La atoms from the high-symmetry positions, respectively. (c) The series of (042) planes that comprise the o sublattice, with the a axis normal to the page. The t sites are excluded for clarity.

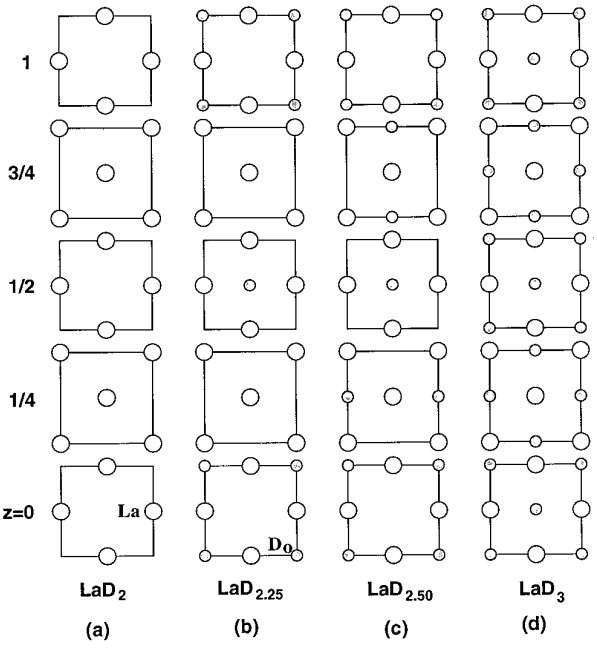

FIG. 3. Selected basal-plane slices of the LaD_{2+x} unit cells (x = 0, 0.25, 0.5, and 1) emphasizing the differences in D_o ordering for $LaD_{2.25}$ ($I4/mmm$) and $LaD_{2.50}$ ($I4_1/amd$).

additional occupied (042) plane for $LaD_{2.50}$ ($I4_1/amd$ symmetry) compared to $LaD_{2.25}$ ($I4/mmm$ symmetry) corresponds to the additional half-occupation of o sites in the otherwise empty basal planes at $z = \frac{1}{4}$ and $\frac{3}{4}$. If $LaD_{2.50}$ had a $P4/mmm$ structure wherein every other (042) plane were occupied instead of the observed $I4_1/amd$ structure, then the basal planes at $z = \frac{1}{4}$ and $\frac{3}{4}$ would remain vacant, and the half-occupied basal planes at $z = 0$ and $\frac{1}{2}$ would become fully occupied with the additional D_o atoms. Two-thirds of the nearest-neighbor o sites surrounding each D_o would also be vacant in the $P4/mmm$ structure, as in the $I4_1/amd$ structure. Yet, along the c directions, half of the La atoms would have no nearest-neighbor D_o atoms, and the other half would be straddled by two nearest-neighbor D_o atoms. This arrangement would preclude the possibility of any energy-stabilizing displacements of La atoms toward the D_o atoms, as seen for the $I4_1/amd$ structure. Even without considering such displacements, recent first-principles calculations (25, 27) for hypothetical β-$YH_{2.50}$ have predicted that the $I4_1/amd$ structure is still a more stable ground-state configuration than the $P4/mmm$ structure. This prediction is expected to apply to other rare-earth hydride systems and appears to be related to structure-dependent details of the long-range interactions between H atoms in the lattice.

Throughout the Rietveld refinements, the different deuterium occupancy parameters (n_D) were allowed to vary,

thus providing a refinement-generated check of the supposed sample stoichiometry. The D/La atom ratios determined from the n_D values in Table 2 suggest that our sample may have been slightly D-deficient, i.e., closer to $\sim LaD_{2.48}$, although the data are consistent with a stoichiometry of $LaD_{2.50}$ within the standard uncertainties. In addition, the low-temperature refinement results indicate slight deviations from perfect D_o ordering, even at 10 K. In particular, the 10-K fit shows that, although the D(t) sites are fully occupied, a small percentage (~3%) of the D_o atoms are displaced from the D(o1) sites to randomly occupy some of the D(o2) sites. These deviations probably originate from an intrinsic D_o order–disorder equilibrium that exists at finite temperatures. Cooling the $LaD_{2.50}$ sample below a certain temperature (~200 K) likely freezes-in (on the timescale of the experiment) an order–disorder configuration that is present at slightly higher temperatures. This behavior is in line with electrical resistivity measurements (2, 28, 29) of RH_{2+x} compounds, which typically indicated a freezing-in of H_o disorder in samples rapidly quenched to low temperature from above the order–disorder transition temperature.

The lattice parameters and tetragonality $[(0.5c_T\text{-}a_T)/a_T]$ found for $LaD_{2.50}$ in this NPD study are in mixed agreement with earlier $La(H/D)_{2+x}$ X-ray diffraction (XRD) studies near $x = 0.5$. For example, XRD data for $LaD_{2.46}$ (30) and $LaD_{2.50}$ (31) yielded cubic lattice parameters $a = 5.611(1)$ Å and 5.6168(8) Å, respectively, at room temperature, yet failed to indicate any tetragonal distortions for these samples or their deuterated analogs. These lattice parameters compare well with the value of $a_T = 5.61101(8)$ Å at 300 K found in the present study. A later XRD study (32) of LaH_{2+x} suggested that a tetragonal distortion indeed appears in the vicinity of room temperature for x near 0.5 and persists to low temperatures. The reported tetragonalities were ~0.8% at 213 K and ~0.7% at 118 K. Interpolations of the present $LaD_{2.50}$ results indicate corresponding tetragonalities of ~0.84 and 0.94%, respectively. It is currently unclear what is causing the discrepancies between the different studies concerning the distortional behavior of $LaD_{2.50}$. It may be the result of resolution limitations in the XRD techniques used in the earlier studies or of slight differences in the true D/La stoichiometric ratios among the various studies due to different synthesis procedures and materials used. A variety of preparation factors such as the presence of sample impurities and inhomogeneities can lead to stoichiometric uncertainties that have an impact on the structural properties. Care was taken in the present study to minimize stoichiometric uncertainties, and we again emphasize that the NPD results corroborated the targeted D/La stoichiometry within the standard uncertainties.

The temperature-dependent behavior of selected $LaD_{2.50}$ physical properties are summarized in Figs. 4a and 4b. Extrapolation of the $LaD_{2.50}$ data in Figs. 4a and 4b indicate that the onset of D_o ordering and the accompanying tetragonal distortion occurs at 385(5) K. The slight maximum in c_T at ~200 K [11.2951(2) Å] coincides with the attainment of nearly perfect long-range order. Below 200 K, c_T increases with temperature, indicative of normal thermal expansion. Between 200 and 385 K, c_T decreases with temperature, coinciding with a decrease in the degree of long-range order. Above 385 K, c_T for the disordered phase increases with temperature, again indicative of normal thermal expansion. The perturbations of long-range ordering on a_T appear to be much less dramatic, with the increase in a_T with temperature apparently dominated by thermal expansion effects over the entire range measured. The different temperature-dependent behaviors of a_T and c_T lead to a tetragonality that becomes maximized at low temperature [0.948(3)% at 10 K]. The D(t) site occupancies, which were allowed to vary during the refinements, confirm that the t sites are essentially filled, up to a temperature of ~350 K, above which ~1–2% of the t sites may become vacated over the temperature range investigated. This is in contrast to the earlier NPD studies of $LaD_{2.30}$ (9) and $NdD_{2.36}$ (10), which reported t-site vacancy fractions already near 6 and 7%, respectively, at room temperature. Unlike the fully occupied D(t) sites in the present study, the gradual increase and decrease in D(o1) and D(o2) site occupations, respectively, upon lowering the temperature below 385 K are reminiscent of a second-order phase transition. This is in line with the predictions of static-concentration-waves theory that was used to describe the ordering processes in CeH_{2+x} for $0.35 < x < 0.65$ (33, 34).

It is interesting to compare the temperature-dependent behavior of the lattice parameters, tetragonality, and deuterium site occupancies for $LaD_{2.50}$ with that reported previously for $CeD_{2.45}$ (11). The corresponding $CeD_{2.45}$ data are summarized in Figs. 4c and 4d. The $CeD_{2.45}$ data also exhibit an $I4_1/amd$ structure with a transition temperature of 398 K. Moreover, the temperature dependences of the D(o1) and D(o2) site occupancies for $CeD_{2.45}$ display a similar second-order behavior. (N.B., the D site occupancies were determined assuming $n_{D(t)} = 1$ at all temperatures and $n_{D(o2)} = 0$ below 300 K.) Yet, the lattice parameters and tetragonal distortion for $CeD_{2.45}$ display somewhat different temperature-dependent behavior than for $LaD_{2.50}$. In particular, c_T is maximized at around 300 K [11.1138(1) Å], below which there is a much larger drop in c_T than is attributable to normal thermal effects. Moreover, a_T exhibits a minimum at ~100 K [5.51909(7) Å], unlike for $LaD_{2.50}$, which is also unattributable to normal thermal effects. This anomalous behavior may be an indication of additional phase transitions occurring at lower temperatures below 300 K. Indeed, the predictions of static-concentration-waves theory for CeH_{2+x} have suggested (34) that, besides the higher-temperature, second-order,

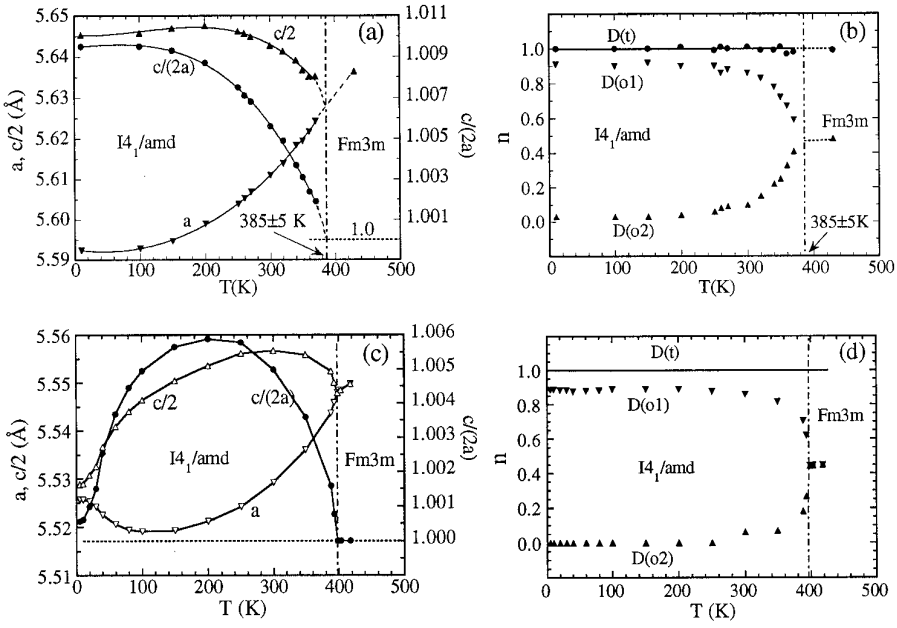

FIG. 4. Comparison of the temperature-dependent behavior of the lattice parameters, tetragonality, and deuterium site occupancies for (a) and (b) $LaD_{2.50}$ (this work) and (c) and (d) $CeD_{2.45}$ (11).

order–disorder phase transition for $0.35 < x < 0.65$, an additional order–order transition exists at lower temperature, which has a two-step character, including first- and second-order parts, for $0.45 \leq x < 0.56$. A similar theoretical analysis of the LaH_{2+x} system (35) has led to different conclusions concerning the LaH_{2+x} phase diagram, indicating no additional lower-temperature phase transitions for $LaH_{2.50}$, as suggested by the present NPD data.

Differential thermal analysis (36) of $CeH_{2.46}$ and differential scanning calorimetry (DSC) measurements (37) for $CeH_{2.47}$ indicated definite thermal effects near room temperature, which were believed to be associated with a transition to the ordered state from a two-phase, order–disorder region at higher temperatures. Later, additional DSC measurements (1) for LaH_{2+x} and CeH_{2+x} led to the construction of similar phase diagrams for the two systems, again suggesting the presence of a two-phase region above room temperature for x near 0.5. Corresponding XRD measurements (1, 32) were in mixed agreement. Although XRD data for CeH_{2+x} near $x = 0.5$ were qualitatively consistent with the DSC results, XRD data for LaH_{2+x} near $x = 0.5$ failed to clearly corroborate any two-phase region of stability suggested by the DSC results above room temperature. The $LaD_{2.50}$ and $CeD_{2.45}$ NPD data are both inconsistent with a two-phase region that involves a mixture of disordered (*Fm*3*m*) cubic and ordered (*I*4/*mmm*) tetragonal phases as suggested by the DSC-generated LaH_{2+x} and CeH_{2+x} phase diagrams. In particular, for the $LaD_{2.50}$ data, no Bragg peaks corresponding to the $(002)_T$ and $(310)_T$ reflections, which are representative of the presence of *I*4/*mmm* symmetry (5), were evident over the entire temperature range measured. An extra effort was taken to measure $LaD_{2.50}$ powder patterns in 2-K steps between 258 and 270 K (see Tables 1–3) in order to investigate the DSC-determined (1) phase-transition temperature at ~265 K. Electrical resistivity measurements reported for $LaH_{2.49}$ (38) were also suggestive of a phase-transition temperature in this region. Although there are some hints of slight deviations from the overall temperature-dependent behavior of the various $LaD_{2.50}$ physical properties [e.g., the slight ripple in the D(o1) and D(o2) site-occupancy plots in the 260 to 270-K region in Fig. 4b], these deviations are within the standard uncertainties of the refinement parameters. Therefore, unless the predicted phase-diagram boundary at ~265 K is due to some subtle structural change within the *I*4$_1$/*amd* symmetry group, it appears that the true boundary is located at a somewhat lower temperature in the vicinity of 200 to 230 K and marks the completion of the long-range D_o structural ordering which begins at ~385 K.

SUMMARY

An NPD study of the structure of $LaD_{2.50}$ was undertaken between 10 and 430 K. Rietveld refinements indicated that the structure possesses cubic *Fm*3*m* symmetry above ~385 K, with D atoms fully occupying the interstitial

t sites of the fcc La lattice and the excess D atoms randomly occupying a portion of the interstitial o sites. Below ~385 K, the structure possesses tetragonal $I4_1/amd$ symmetry concomitant with a D_o long-range order that is fully developed by ~200–230 K. Perfect long-range order can be described as a repeating four-plane sequence comprised of two consecutive (042) planes with fully occupied o sites followed by two consecutive (042) planes with fully vacant o sites. This ordering is accompanied by basal-plane displacements of the D_t atoms in a correlated fashion along either the *a* or *b* axes as well as *c*-directed displacements of the La atoms toward the D_o atoms. The observed structural behavior is similar to that reported previously for the light-rare-earth deuterides RD_{2+x} for $0.3 < x < 0.5$, although differences in the temperature-dependent behaviors of the lattice constants for $LaD_{2.50}$ and $CeD_{2.45}$ may very well signal subtle yet fundamental differences in the structural details of these two compounds in the low-temperature regime.

ACKNOWLEDGMENTS

The authors thank P. Vajda and I. G. Ratishvili for helpful discussion.

REFERENCES

1. K. Conder, L. Wang, E. Boroch, E. Kaldis, and J. Schefer, *Eur. J. Solid State Inorg. Chem.* **28,** 487 (1991).
2. J. N. Daou, J. P. Burger, and P. Vajda, *Philos. Mag. B* **65,** 127 (1992).
3. C. Ohki, H. Uchida, and Y. C. Huang, *Z. Phys. Chem. N. F.* **163,** 149 (1989).
4. M. H. Mintz, Z. Hadari, and M. Bixon, *J. Less-Common Met.* **37,** 331 (1974).
5. T. J. Udovic, Q. Huang, J. J. Rush, J. Schefer, and I. S. Anderson, *Phys. Rev. B* **51,** 12116 (1995).
6. V. K. Fedotov, V. G. Fedotov, M. E. Kost, and E. G. Ponyatovskii, *Sov. Phys. Solid State* **24,** 1252 (1982). [*Fiz. Tverd. Tela* (*Leningrad*) **24,** 2201 (1982).]
7. G. André, O. Blaschko, W. Schwarz, J. N. Daou, and P. Vajda, *Phys. Rev. B* **46,** 8644 (1992).
8. Q. Huang, T. J. Udovic, J. J. Rush, J. Schefer, and I. S. Anderson, *J. Alloys Compounds* in press.
9. C. G. Titcomb, A. K. Cheetham, and B. E. F. Fender, *J. Phys. C* **7,** 2409 (1974).
10. P. Knappe, H. Müller, and H. W. Mayer, *J. Less-Common Met.* **95,** 323 (1983).
11. R. R. Arons, *in* ''Landolt-Börnstein, New Series III'' (H. P. J. Wijn, Ed.), Vol. 19d1, p. 280. Springer-Verlag, Berlin, 1991.
12. P. Vajda, J. N. Daou, and J. P. Burger, *Phys. Rev. B* **36,** 8669 (1987).
13. T. J. Udovic, J. J. Rush, and I. S. Anderson, *Phys. Rev. B* **50,** 15739 (1994).
14. J. K. Stalick, E. Prince, A. Santoro, I. G. Schroder, and J. J. Rush, *in* ''Neutron Scattering in Materials Science II,'' Mater. Res. Soc. Symp. Proc. (D. A. Neumann, T. P. Russell, and B. J. Wuensch, Eds.), Vol. 376, Materials Research Society, Pittsburgh, PA, in press.
15. H. M. Rietveld, *J. Appl. Crystallogr.* **2,** 65 (1969).
16. A. C. Larson and R. B. Von Dreele, ''General Structure Analysis System,'' University of California, Berkley, 1985.
17. J. Schefer, P. Fischer, W. Hälg, J. Osterwalder, L. Schlapbach, and J. D. Jorgensen, *J. Phys. C: Solid State Phys.* **17,** 1575 (1984).
18. A. K. Cheetham and B. E. F. Fender, *J. Phys. C* **5,** L35 (1972).
19. P. Fischer, W. Hälg, L. Schlapbach, and K. Yvon, *J. Less-Common Met.* **60,** 1 (1978).
20. J.-J. Didisheim, K. Yvon, P. Fischer, W. Hälg, and L. Schlapbach, *Phys. Lett.* **78A,** 111 (1980).
21. T. J. Udovic, Q. Huang, and J. J. Rush, *J. Phys. Chem. Solids*, in press.
22. T. J. Udovic, J. J. Rush, and I. S. Anderson, *Phys. Rev. B* **50,** 7144 (1994).
23. T. J. Udovic, J. J. Rush, and I. S. Anderson, *J. Alloys Compounds,* in press.
24. T. J. Udovic, J. J. Rush, and I. S. Anderson, *J. Phys.: Condens. Matter.* **7,** 7005 (1995).
25. Y. Wang and M. Y. Chou, *Phys. Rev. B* **49,** 10731 (1994).
26. P. Vajda, J. N. Daou, and G. Andre, *Phys. Rev. B* **48,** 6116 (1993).
27. S. N. Sun, Y. Wang, and M. Y. Chou, *Phys. Rev. B* **49,** 6481 (1994).
28. J. P. Burger, J. N. Daou, and P. Vajda, *Philos. Mag. B* **58,** 349 (1988).
29. J. P. Burger, P. Vajda, and J. N. Daou, *J. Phys. Chem. Solids* **52,** 779 (1991).
30. H. Müller, P. Knappe, and O. Greis, *Z. Phys. Chem. N. F.* **114,** 45 (1979).
31. P. Klavins, R. N. Shelton, R. G. Barnes, and B. J. Beaudry, *Phys. Rev. B* **29,** 5349 (1984).
32. E. Boroch, K. Conder, C. Ru-Xiu, and E. Kaldis, *J. Less-Common Met.* **156,** 259 (1989).
33. I. G. Ratishvili, P. Vajda, and A. Boukraa, *J. Phys. Chem. Solids* **54,** 1055 (1993).
34. I. G. Ratishvili, P. Vajda, A. Boukraa, and N. Z. Namoradze, *Phys. Rev. B* **49,** 15461 (1994).
35. P. Vajda and I. G. Ratishvili, private communication.
36. I. O. Bashkin, M. E. Kost, and E. G. Ponyatovskii, *Phys. Status Solidi* (*a*) **83,** 461 (1984).
37. E. Boroch and E. Kaldis, *Z. Phys. Chem. N. F.* **163,** 117 (1989).
38. D. K. Misemer and B. N. Harmon, *Phys. Rev. B* **26,** 5634 (1982).